ELSEVIER

Journal of Photochemistry and Photobiology A: Chemistry 107 (1997) 215–220

Journal of PHOTOCHEMISTRY AND PHOTOBIOLOGY A: CHEMISTRY

Photocatalytic reduction of nitrite and nitrate ions over doped TiO_2 catalysts

K.T. Ranjit, B. Viswanathan *

Department of Chemistry, Indian Institute of Technology, Madras, India

Received 23 October 1996; accepted 19 January 1997

Abstract

Doping of TiO_2 with altervalent cations, Fe^{3+}, Cr^{3+}, Co^{2+} and Mg^{2+} leads to a red shift in the onset of absorption. The role of the dopant ions is primarily to improve the charge separation by means of a permanent electric field. Doping of TiO_2 also influences the adsorption of reagent species and the resulting photoactivity is a consequence of these two factors. An optimum level of dopant ions is beneficial for the photocatalytic activity of TiO_2. © 1997 Elsevier Science S.A.

Keywords: Photocatalytic reduction; Doped TiO_2 catalysts; Reduction of nitrate and nitrite ions

1. Introduction

Although many semiconducting oxides have been investigated as potential photocatalysts [1–5], TiO_2 has been shown to be the most suitable material, offering the highest light conversion efficiency, mainly because of its stability under irradiation conditions and its relatively favorable band-gap energy. Attempts to improve the performance of TiO_2 as a photocatalyst under UV illumination and to extend its light absorption and conversion capacity to visible portion of the solar spectrum have primarily been concentrated with the effect of dopants [6–13].

The reduction of nitrate ions has receive considerable attention over the last years. The reduction of nitrate is of interest as a means of mimicking reduction of nitrogen oxyanion substrates in nature and developing novel nitrogen fixation systems [14,15]. The reduction of nitrogen oxides and oxyanions has been extensively studied electrochemically [16], biochemically [17,18] and catalytically [19]. However reports of photocatalytic reduction of nitrogen oxyanion are scarce [20–24].

Herein we report the photocatalytic reduction of nitrite and nitrate ions to ammonia over doped TiO_2 catalysts.

2. Experimental

2.1. Preparation of doped TiO_2

Pure TiO_2 was prepared either by a sol–gel process or by the hydrolysis of $TiCl_4$. The resulting solid was dried at 393 K for 24 h and then fired in air at 823 K for 24 h since crystallization to anatase phase occurred only under these pretreatment conditions. The doped samples were prepared by impregnation method. The metal salt solution required for the loading was added to a known weight of TiO_2 in such a way that it wets the TiO_2 completely. The slurry was stirred at ambient temperature overnight and dried in an air oven at 383 K for 12 h. The dried powder was heated from room temperature to 673 K in hydrogen atmosphere, maintained at 673 K for 12 h and cooled to room temperature in hydrogen atmosphere. The prepared catalysts were stored in vacuum desiccators.

2.2. Estimation of metal loading

The dopant concentration in the catalysts were analyzed using an inductively coupled plasma atomic emission spectrometer (ICPAES, Model 3410, ARL) after calibration with standard solution containing metal solution.

2.3. X-ray diffraction (XRD) studies

X-ray diffractograms were obtained for the powdered samples with a Phillips diffractometer (Phillips Generator, Hol-

* Corresponding author. Tel: +91 44 235 1365; fax: +91 44 235 0509.

PII S1010-6030(97)00025-7

land: Model PW 1130) provided with an online recorder and dot-matrix printer (Tele type, USA). The diffraction patterns were recorded at room temperature using Ni filtered Cu Kα radiation ($\lambda = 1.5418$ Å) for all the samples. A scanning speed of 3 deg min^{-1} and a chart speed of 5 mm deg^{-1} were generally employed.

2.4. Thermogravimetry (TG)–differential scanning calorimetry (DSC)

TG–DSC experiments of some of the catalysts were carried out in a Perkin-Elmer (TGA-DSC-7) instrument in the temperature range 322–873 K for TG studies and 323–773 K for DSC studies, under air. A flow rate of 20 ml min^{-1} and a heating rate of 20 °C min^{-1} were usually employed for all the samples.

2.5. Surface area studies

The surface area of the samples was measured by N_2 adsorption at 77 K using the dynamic BET method using a Carlo Erba (model 1800) sorptometer. The samples were outgassed in an evacuation chamber to a pressure of 10^{-3} atm at 393 K prior to adsorption.

2.6. Diffuse reflectance spectroscopic studies

A Hitachi spectrophotometer (model 150-20) equipped with an integrating sphere was used to record the diffuse reflectance spectra of the samples. The base line correction was done using a calibrated sample of barium sulphate. The spectra were recorded at room temperature in air in the range 350–900 nm. The same spectrophotometer was used for recording the UV absorption spectra of solutions.

2.7. Photocatalytic studies

The photocatalytic experiments were performed in an all glass static system at ambient temperature and atmospheric pressure. In all the experiments, 100 mg of the freshly prepared catalyst and 20 ml of the appropriate solution (sodium nitrite and sodium nitrate of appropriate concentration for nitrite and nitrate reduction) was taken in a double walled cylindrical Pyrex glass reactor. The reactor was equipped with water circulation in the outer jacket in order to maintain a constant temperature as well as for IR filtering. The reaction mixture was stirred at a constant speed during illumination by a magnetic stirrer. The suspension was irradiated using a 450 W Xe lamp (Oriel Corporation, USA). Argon gas was purged when nitrite (nitrate) solutions were illuminated. Before starting the illumination, the reaction mixture was stirred for half an hour in the dark. After irradiation the solution was centrifuged to remove essentially all the catalyst and the centrifugate was analyzed for ammonia.

2.8. Estimation of ammonia

Ammonia was estimated by the indophenol-blue method [25].

3. Results and discussion

3.1. Iron doped catalysts

The X-ray diffraction pattern of the iron doped samples showed peaks corresponding to anatase phase of TiO_2 only. No peaks due to haematite (Fe_2O_3) are observed in any of these samples. Hence it is concluded that the incorporation of iron in these catalysts does not catalyze the anatase to rutile phase transformation at least at the temperatures at which these catalysts were calcined. TG analysis and DSC studies showed a small endothermic peak at ≈723 K. This is due to the decomposition of the adsorbed nitrate, which is used as the precursor. These results corroborate the fact that no rutile phase is present in these catalysts. The characteristics of the iron doped samples are given in Table 1.

From Table 1 it is clear that with increasing iron content there is an increase in the unit cell volume, but beyond a certain value the unit cell volume decreases. The ionic radius of Fe^{3+} is 0.64 Å while that of Ti^{4+} is 0.68 Å. The increase in unit cell volume indicates that Fe^{3+} does not replace Ti^{4+} in the lattice but forms a solid solution. The diffuse reflectance spectra of the specimens showed that the onset of absorption was shifted to longer wavelengths with increase in iron content. In addition, the absorbance of the samples was found to increase with increase in iron content. However, no tail-end absorption was found in the visible region for all the impregnated samples. The onset of absorption as a function of iron content is given in Table 2.

The photocatalytic activity was examined on the iron doped TiO_2 catalysts and the results obtained are given in Table 3.

It is observed that the yield of ammonia (expressed per unit surface area) decreases monotonically with increase of

Table 1
Characteristics of doped samples

Dopant	Dopant content (wt.%)	Surface area ($m^2 g^{-1}$)	Unit cell volume (Å^3)
Iron	0.04	21.1	136.47
	0.06	14.8	136.58
	0.10	19.3	136.58
	0.33	12.8	136.42
Chromium	0.09	17.5	136.65
	0.16	18.2	136.54
	0.19	15.4	137.13
	0.23	15.2	136.49
Cobalt	0.15	14.4	136.53
	0.25	16.6	136.41
	0.98	14.6	136.27

Table 2
Onset of absorption vs. the iron content for iron doped catalysts

Fe content (wt.%)	Onset of absorption (nm)
0.04	388
0.06	392
0.10	400
0.33	412

iron content. However, the pure TiO_2 did not exhibit any activity. Thus, the increase in activity on doping with iron can be attributed to the increase in the life time of electron–hole pairs. Another important factor that affects the photocatalytic activity is the equilibrium dark adsorption of the reagent species. The extent of equilibrium adsorption of nitrite was evaluated from ΔC, the decrease in nitrite concentration in 20 ml aliquots of solution after equilibration under stirring conditions for 4 h with 100 mg of the semiconductor. The extents of adsorption are expressed in a normalized form, i.e. the number of moles adsorbed per gram of the catalyst, n_2^s, and calculated using the expression, $n_2^s = \Delta C\, V/10^3 w$, where ΔC is the decrease in nitrite concentration, V is the volume of the solution and w is the weight of the catalyst used. It was found that the equilibrium dark adsorption of nitrite was higher on iron doped TiO_2 catalysts compared with pure TiO_2 catalyst. Thus, the resulting photoactivity is a combination of the above mentioned two factors.

3.2. Chromium doped catalysts

The system formed by chromium doped polycrystalline titania has been widely studied in the field of photocatalysis [7]. The role of Cr^{III} ions used as dopant for TiO_2 is mainly to improve the charge separation of the photoproduced electron–hole pairs by means of a permanent electric field. Hence, chromium doped TiO_2 catalysts were evaluated for the photocatalytic reduction of nitrite and nitrate ions.

The X-ray patterns of all the samples show lines corresponding to the anatase phase only. This result has been corroborated by TG analysis and DSC studies. No exotherm was observed in all the samples ruling out any phase transformations.

The ionic radius of Ti^{4+} is 0.68 Å while that of Cr^{3+} is 0.62 Å. The lattice parameters calculated show that there is no systematic variation in the unit cell volume with increasing chromium content. However, the doped catalysts have a larger unit cell volume than the bare TiO_2 semiconductor. This suggests that Cr^{3+} does not replace Ti^{4+} in the lattice but forms a solid solution. The characteristics of the chromium doped TiO_2 specimens are given in Table 1.

The diffuse reflectance spectra of the specimens showed that the onset of absorption was shifted to longer wavelengths with increase in chromium content (Fig. 1). For the sample containing 0.23% Cr, a broad band with a maximum centered around 600 nm is observed. This is attributed to the spin allowed d–d transition ($^4A_{2g} \rightarrow {}^4T_{2g}$) of Cr^{3+} in an octahedral environment. In addition, the absorbance at wavelengths ≤ 400 nm was found to increase with increase in chromium content.

The chromium doped samples were evaluated for the photocatalytic reduction of nitrite and nitrate ions to ammonia and the results are given in Table 3.

The opposite trends observed in photocatalytic activity with iron (continuous decrease with increase of iron content) and chromium (increase with increase of chromium content) doping can be associated with the lifetimes of the charge carriers because of the differences in the space charge region produced. However, it is not certain whether this factor alone is responsible or whether other factors also contribute to the differences observed.

Table 3
Photocatalytic activity of doped TiO_2 catalysts

Dopant	Dopant concentration (wt.%)	Yield of ammonia (μmol)	
		$NO_2^- \rightarrow NH_3$	$NO_3^- \rightarrow NH_3$
Iron	0.04	0.67	0.31
	0.06	0.36	0.17
	0.10	0.42	0.24
	0.33	0.13	0.04
Chromium	0.09	0.07	0.11
	0.16	0.19	0.15
	0.19	0.17	0.41
	0.23	0.25	0.38
Cobalt	0.15	0.24	0.67
	0.25	0.37	0.96
	0.98	0.15	0.22
Magnesium	0.53	0.35	0.21
	1.41	0.55	0.31
	2.94	0.30	0.14

Reaction conditions: 20 ml of 10 ppm nitrite (nitrate), 2 h irradiation, 100 mg catalyst.

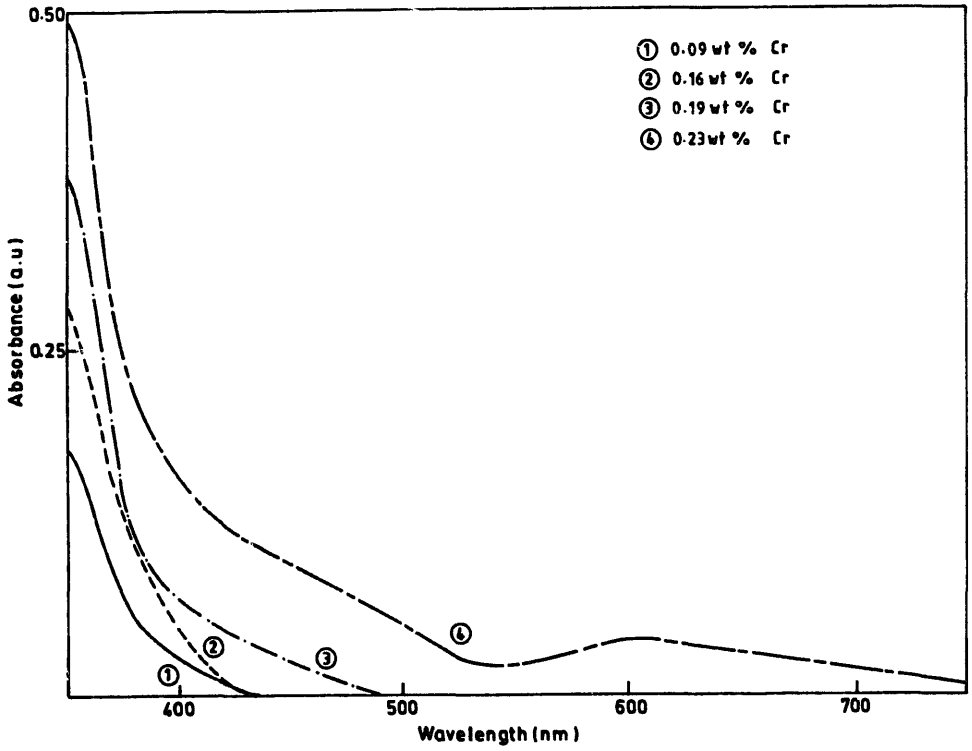

Fig. 1. Diffuse reflectance spectra of chromium doped TiO_2 catalysts.

3.3. Cobalt doped catalysts

Little work has been reported on incorporating cobalt metal ion. The ionic radius of Co^{2+} is 0.74 Å while that of Ti^{4+} is 0.68 Å. Hence, cobalt doped TiO_2 catalysts were examined in detail.

The X-ray patterns of all the samples show lines corresponding to anatase phase only. This result was corroborated by DSC studies. No exotherm was observed in all the samples ruling out any phase transformation. The lack of diffraction peaks due to cobalt oxide may be attributed to the fact that cobalt species are randomly dispersed on the TiO_2 surface. The characteristics of cobalt doped catalysts are given in Table 1.

There is a progressive decrease in the unit cell volume with increase in cobalt content, although the ionic radius of Co^{2+} is larger than that of Ti^{4+}. This suggests Co^{2+} does not replace Ti^{4+} in a substitutional or interstitial position in the lattice but rather forms a solid solution.

The diffuse reflectance spectra of the specimens are shown in Fig. 2. The onset of absorption is shifted to longer wavelengths with increase in cobalt content. In addition, the absorbance of the samples is found to increase with increase in cobalt content. The photocatalytic reduction of nitrite and nitrate was evaluated on cobalt doped TiO_2 catalysts. The results are given in Table 3.

Doping of TiO_2 with altervalent cations such as cobalt results in increased concentration of holes in the valence band as expected from the defect site reaction involving one Ti ion and one CoO species.

Thus the flatband potential shifts anodically on doping with a lower valent cation. An increase of the dopant ion content, however, favors the efficiency of the electron–hole separation and then the photoactivity. The thickness of the space charge layer decreases as the dopant content increases. The electron–hole pairs photogenerated within the region are efficiently separated by the large electric field traversing the barrier, before having the chance to recombine. However as the hole-concentration is increased, the surface barrier is lowered further and the space charge region becomes progressively thicker. The transient time across the barrier is increased and the probability of the carriers recombining is increased. Consequently, it is understandable that there exists an optimal value at which the photoactivity is maximum.

3.4. Magnesium doped catalysts

Mg doping has been shown to enhance the water cleavage process and photo-uptake of oxygen [8]. In the present investigation, the photocatalytic reduction of nitrite and nitrate ions was evaluated on magnesium doped TiO_2 catalysts.

All the calcined catalysts showed peaks due to the anatase phase of TiO_2 only. The lack of detection of MgO diffraction pattern indicate that magnesium species are randomly dispersed on the TiO_2 surface.

The diffuse reflectance spectra of Mg doped catalysts showed that the onset of absorption was shifted marginally to longer wavelength with increase in magnesium content. Also the calcination temperature was found to affect the absorbance of the samples. However, no tail-end absorbance

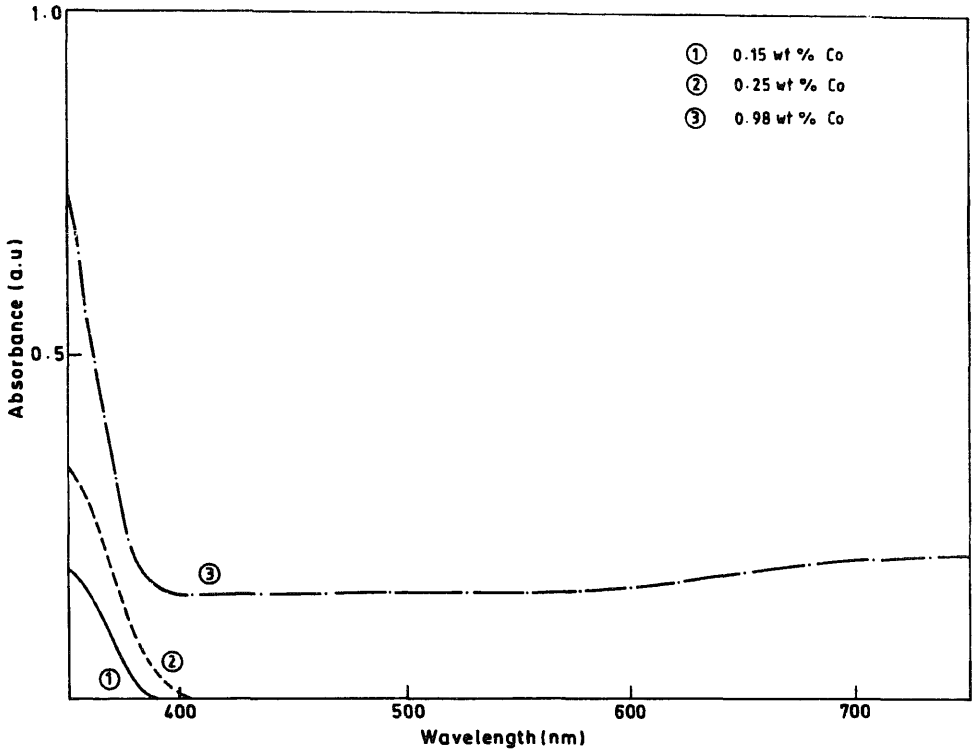

Fig. 2. Diffuse reflectance spectra of cobalt doped TiO_2 catalysts.

was found in the visible region from 500 to 900 nm in all the magnesium doped catalysts.

The characteristics of magnesium doped catalysts and the onset of absorption are given in Table 4.

From Table 4 it is clear that the onset of absorption is shifted marginally or is almost constant with increase in calcination temperature. However, there was an increase in the absorbance at wavelengths ≤ 400 nm with increase in calcination temperature. Similarly the catalysts containing 1.41 wt.% and 2.94 wt.% magnesium had onset of absorption at 405 nm and 428 nm respectively.

The photocatalytic reduction of nitrite and nitrate ions was evaluated over magnesium doped TiO_2 catalysts and the results are given Table 3.

The optimum calcination temperature was found to be 873 K for the magnesium doped catalysts and hence all the samples were calcined at this temperature. We see from Table 3 that an optimum magnesium content is beneficial for the photoactivity. A similar explanation given for cobalt doped TiO_2 catalyst is applicable for Mg doped TiO_2 catalysts. An optimal value of donor atoms is necessary for which a space charge region exists, and whose thickness is more or less equal to the light penetration depth.

Table 4
Characteristics of magnesium doped (0.53 wt.%) catalyst

Calcination temperature (K)	Surface area ($m^2 g^{-1}$)	Onset of absorption
673	13.4	389
773	16.3	390
873	22.6	392
973	14.9	394
1073	10.8	400

4. Conclusions

1. The calcination temperature employed in the present study does not allow the dopant ions to diffuse into the bulk. The lack of detection of oxide peaks of dopant ions indicate that these ions are dispersed randomly on the TiO_2 surface. The probable picture is that a solid solution is formed involving few layers. The lattice parameters calculated corroborate this point.
2. The onset of absorption is shifted to longer wavelengths on doping TiO_2 with altervalent cations. Also, the absorbance values increase, with increase in dopant concentration.
3. The role of dopant ion is primarily to improve the charge separation of the photoproduced electron–hole pairs by means of a permanent electric field.
4. An increase in dopant ion content favors the efficiency of the electron–hole separation and then the photoactivity. But beyond a certain level, the space charge layer becomes thicker and hence the probability of the carriers recombining is increased. Thus there is an optimal value at which photoactivity is maximum.
5. Doping of TiO_2 could influence the adsorption of the reagent species (the equilibrium dark adsorption of nitrite was found to be higher for doped catalysts compared to pure TiO_2) and this is another important factor which leads to the enhanced activity of the doped catalysts.

References

[1] K. Kalyanasundaram, E. Borgarello, M. Grätzel, Helv. Chim. Acta 64 (1981) 362.
[2] A. Kudo, A. Tanaka, K. Domen, K.i.-Maruya, K.I. Aika, T. Onishi, J. Catal. 111 (1980) 67.
[3] G.A. Somorjai, M. Hendewerk, J.E. Turner, Catal. Rev. Sci. Eng. 26 (1984) 683.
[4] S. Sato, J.M. White, J. Phys. Chem. 85 (1981) 592.
[5] J. Kiwi, M. Grätzel, J. Phys. Chem. 88 (1984) 1302.
[6] H.P. Maruska, A.K. Ghosh, Sol. Energy Mater. 1 (1979) 237.
[7] E. Borgarello, J. Kiwi, M. Grätzel, E. Pelizzetti, M. Visca, J. Am. Chem. Soc. 104 (1982) 2996.
[8] J. Kiwi, M. Grätzel, J. Phys. Chem. 90 (1986) 637.
[9] E. Borgarello, J. Kiwi, E. Pelizzetti, M. Visca, M. Grätzel, J. Am. Chem. Soc. 103 (1981) 6324.
[10] J. Kiwi, C. Morrison, J. Phys. Chem. 88 (1984) 6146.
[11] W.K. Wong, M.A. Malati, Sol. Energy 2 (1986) 163.
[12] A. Davidson, M. Che, J. Phys. Chem. 96 (1992) 9909.
[13] M.M.- Hukovic, M.C.- Ceric, Mater. Res. Bull. 23 (1988) 1535.
[14] J. Chatt, J.R. Dilworth, R.L. Richards, Chem. Rev. 78 (1978) 589.
[15] I. Willner, N. Lapidot, A. Riklin, J. Am. Chem. Soc. 111 (1989) 1883.
[16] X. Xing, D.A. Scherson, C. Mak, J. Electrochem. Soc. 137 (1990) 2166.
[17] M. Losada, J. Mol. Catal. 1 (1975) 245.
[18] A. Scherer, R.K. Thauer, Eur. J. Biochem. 85 (1978) 125.
[19] M. Shelef, Catal. Rev. 11 (1975) 1.
[20] M. Halmann, K. Zuckerman, J. Chem. Soc. Chem. Commun. 455 (1986).
[21] M. Halmann, J. Tobin, K. Zuckerman, J. Electrochem. Soc. 209 (1986) 405.
[22] K.T. Ranjit, R. Krishnamoorthy, B. Viswanathan, J. Photochem. Photobiol. A: Chem. 81 (1994) 55.
[23] K.T. Ranjit, R. Krishnamoorthy, T.K. Varadarajan, B. Viswanathan, J. Photochem. Photobiol. A: Chem. 86 (1995) 185.
[24] K.T. Ranjit, T.K. Varadarajan, B. Viswanathan, J. Photochem. Photobiol. A: Chem. 89 (1995) 67.
[25] D.F. Boltz, J.A. Howell, Colorimetric Determination of Non-Metals, Wiley, New York, 1978, p. 210.